# Analysis of non ambiguous BOC signal acquisition performance Acquisition

Vincent Heiries, Daniel Roviras, Lionel Ries, Vincent Calmettes

# Analysis of Non Ambiguous BOC Signal Acquisition Performance

Vincent Heiries, *TeSA*
Daniel Roviras, *TeSA*
Lionel Ries, *CNES*
Vincent Calmettes, *ENSAE*

## BIOGRAPHY

Vincent Heiries is graduated from ENAC (Toulouse, France). Since September 2003, he is working on new Galileo signal processing in TéSA (Toulouse) as a PhD student.

D. Roviras got his Engineer degree from Ecole Supérieure d'Electricité in 1981. He joined the Electronics Laboratory of ENSEEIHT in 1986, and got his Ph.D. degree from INPT in 1989. He is Full Professor since 1999. His research activities are centered on Communication topics.

Lionel Ries is graduated from the "Ecole Polytechnique de Bruxelles" and received a M.S. degree from SUPAERO (ENSAE, Toulouse, France). He is a Navigation Engineer in the Radionavigation Department at CNES. He is responsible for research activities on GNSS2 signals, including BOC modulations and GPSIIF-L5.

Vincent Calmettes is at the head of the Laboratory of Electronics and Physics, at SUPAERO. His work includes the research, for applications in Digital communications and Signal processing, of solutions with DSP processors and Programmable logic devices or ASICs.

## ABSTRACT

The Binary Offset Carrier planned for future GNSS signals, including several GALILEO signals as well as GPS M-code, presents a high degree of spectral separation from conventional signals. It also greatly improves positioning accuracy and enhances multipath rejection.
However, with such a modulation, the acquisition process is made more complex. Specific techniques must be employed in order to avoid unacceptable errors.
This paper assesses the performance of three methods allowing to acquire and track a BOC signal unambiguously : the Bump-Jumping technique, the "BPSK-like" technique, and the Sub Carrier Phase Cancellation (SCPC) technique. A detailed study of these methods is developed taking into accounts the filtering effects. In order to validate the theoretical results, intensive simulations have been carried out and performance of BOC signal acquisition for the different methods have been assessed and compared with initial theoretical analysis.

## INTRODUCTION

Although more precise in standard conditions, BOC modulation brings some drawbacks, especially associated with the characteristic autocorrelation function. The autocorrelation function of the BOC signal has multiple positive and negative peaks. This characteristic makes a receiver tracking BOC signals more sensitive to dynamic stresses especially. This complicates signal acquisition and tracking, the risk of miss-detection or wrong peak selection being higher. The receiver must ensure that the correct peak is acquired and subsequently tracked. Acquiring and maintaining the correct autocorrelation peak can be a challenge especially in the presence of noise and multipath. However, if the delay lock loop is set up to track the narrow central peak, the accuracy is better than for the corresponding BPSK signal.
Several techniques can be used to get rid of some of the BOC associated problems. We consider the BOC signal processing is sequentially done along three steps. This approach is described in [1]. The first step is the energy search. It makes the local code position sweeping the uncertainty time and frequency domain until energy is detected, which means a correlation peak is present. In this first step, the ACF of the BOC needs to be unambiguous, the specific techniques are used. At the conclusion of this initial acquisition process, the timing accuracy (even at high SNR values) is limited by the search step size. The estimated delay is not necessary within the pull-in range of the code tracking loop. So, we can use a code tracking loop maintaining the method used to make the ACF of the BOC unambiguous to solve this remaining uncertainty along a second step, the transition to tracking stage. Finally, once the convergence is achieved with enough confi-

dence, the receiver turns back to traditional BOC processing, and locks on the main peak, due to accurate positioning of locally generated code enabled by the dedicated transition technique.
This document presents first a theoretical analysis of the three methods studied here. The signal terms and noise term at the output of the receiver are analytically expressed. The expression of detection probability and false alarm probability are given. The error variance of the code tracking loop in transition stage is also calculated. Finally, this paper presents simulations results about the performance of these acquisition techniques along the energy search step and transition to tracking step.

## THE "BPSK-like" METHOD

### First approach : Dual Sideband technique

This technique already studied in the literature can be used both for the energy search and the transition to tracking stages. As it is described in [2], this technique only consists in considering the received BOC(N, M) signal as the sum of two BPSK(M) signals with carrier frequency symmetrically positioned on each side of the BOC carrier frequency. Thus, each lobe is processed separately as a BPSK(M) signal. Indeed, each lobe is filtered out, relocated at the center of the band, and the resulting signal is correlated with a local BPSK(M) reference. The receiver has two correlation channels, one for the upper filtered sideband and one for the lower filtered sideband. On each correlation channel an unambiguous correlation function is provided. The two channels are then combined. Depending on the degree of receiver filtering, the shape of the ACF (on the upper and lower sideband) is well approximated by the magnitude squared ACF of the corresponding ACF of the BPSK signal.

Now, let us calculate the expression of the signal terms at the output of the correlator. The complex envelope of the received signal is (assuming a dataless channel) :

$$s(t) = \sqrt{C}c(t-\tau).sc(t-\tau).e^{j\phi(t)} \quad (1)$$

with :

$$\phi(t) = 2\pi f_D t + \theta \quad (2)$$

and we note :
$\tau$ is the time delay due to propagation of the signal
$f_D$ is the Doppler frequency
$c(t)$ is the Pseudo-Random Noise (PRN) code
$sc(t)$ is the subcarrier of the BOC signal.
$\sqrt{C}$ is the amplitude of the signal, $C$ being the signal power.
$\phi(t)$ is the phase of the signal

Now, let us calculate the expression of the signal present on each channel. For calculations, we will work here with continuous signal instead of sampled signals that would give the same results. First, the complex envelope of the received signal is produced. Then the upper lobe and lower lobe of this BOC signal are separated respectively by the upper band filter $h_H(t)$ and the lower band filter $h_L(t)$. Finally, these two lobes are shifted at the center of the frequency band in order to be correlated with the BPSK reference signal. $s_H(t)$ and $s_L(t)$ are the two components of the signal filtered.
At the output of the correlator, the signal is :

$$Y_H(t_d) = \frac{1}{T_p}\int_{t_d-T_p}^{t_d} \sqrt{C}s_H(t-\tau)e^{j\phi(t)}c(t-\hat{\tau})e^{j\hat{\phi_H}(t)}dt + n_{Y_H}(t_d) \quad (3)$$

$$Y_L(t_d) = \frac{1}{T_p}\int_{t_d-T_p}^{t_d} \sqrt{C}s_L(t-\tau)e^{j\phi(t)}c(t-\hat{\tau})e^{j\hat{\phi_L}(t)}dt + n_{Y_L}(t_d)$$

with :

$$\begin{aligned} s_H(t) &= [(c.sc) * h_H](t) \quad (4)\\ s_L(t) &= [(c.sc) * h_L](t) \\ \hat{\phi_H}(t) &= 2\pi(-\hat{f_D} - f_{sc})t - \hat{\theta} \\ \hat{\phi_L}(t) &= 2\pi(-\hat{f_D} + f_{sc})t - \hat{\theta} \end{aligned}$$

and :

$$n_{Y_H}(t_d) = \frac{1}{T_p}\int_{t_d-T_p}^{t_d} [n * h_H](t).c(t-\hat{\tau})e^{j\hat{\phi_H}(t)}dt \quad (5)$$

$$n_{Y_L}(t_d) = \frac{1}{T_p}\int_{t_d-T_p}^{t_d} [n * h_L](t).c(t-\hat{\tau})e^{j\hat{\phi_L}(t)}dt$$

After calculations, it can be demonstrated from [4] and [5] that :

$$\begin{aligned} Y_H(t_d) &= \sqrt{C}R_{s_H.r_H}(\varepsilon_\tau)sinc(\pi\Delta f T_p)e^{j\varepsilon_\theta} + n_{Y_H}(t_d) \quad (6)\\ Y_L(t_d) &= \sqrt{C}R_{s_L.r_L}(\varepsilon_\tau)sinc(\pi\Delta f T_p)e^{j\varepsilon_\theta} + n_{Y_L}(t_d) \end{aligned}$$

with :

$$r_H(t) = c(t-\hat{\tau})e^{-j2\pi f_{sp}t} \;;\; r_L(t) = c(t-\hat{\tau})e^{+j2\pi f_{sp}t} \quad (7)$$
$$\text{and } \Delta f = f_D - \hat{f_D} \;;\; \varepsilon_\theta = \theta - \hat{\theta} \;;\; \varepsilon_\tau = \tau - \hat{\tau}$$

$R_{s_H.r_H}(\varepsilon_\tau)$ and $R_{s_L.r_L}(\varepsilon_\tau)$ represent respectively the correlation function between $s_H(t)$ and $r_H(t)$, and the correlation function between $s_L(t)$ and $r_L(t)$; i.e. the correlation functions between the received filtered and relocated signal, and the local BPSK reference signal. For more simplicity, it is further called $R_H(\varepsilon_\tau)$ and $R_L(\varepsilon_\tau)$. Figure 1 shows the correlation of the lower filtered (with ideal filter) sideband of the BOC with the BPSK reference signal and

the autocorrelation of the BPSK reference signal. Correlation losses appear with the first one mainly due to filtering effects.

*Note :* The correlation functions plotted on Figure 1, are in fact the correlation of the waveform of the signals. Indeed, since we consider that PRN code has a sufficiently long period, we consider that its ACF presents only one peak at zero delay and no secondary peak. Thus, the correlation function of the signal can be approximated by the correlation function of the waveform.

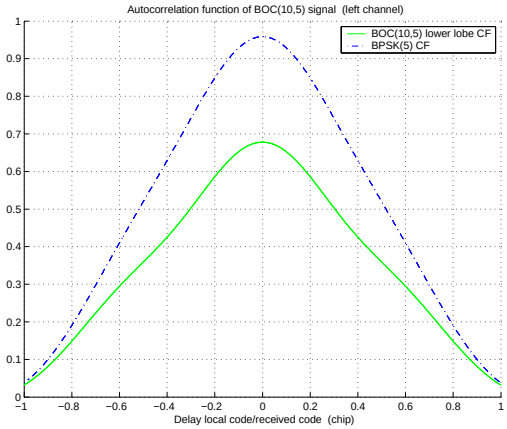


Figure 1: ACF of a BOC(10,5) filtered on the lower band

Finally, we have on the in-phase channel and on the quadrature channel :

$$\begin{aligned} I_H(t_d) &= \sqrt{C}R_H(\varepsilon_\tau)sinc(\pi\Delta f T_p)\cos(\varepsilon_\theta) + n_{I_H}(t_d) \\ Q_H(t_d) &= \sqrt{C}R_H(\varepsilon_\tau)sinc(\pi\Delta f T_p)\sin(\varepsilon_\theta) + n_{Q_H}(t_d) \\ I_L(t_d) &= \sqrt{C}R_L(\varepsilon_\tau)sinc(\pi\Delta f T_p)\cos(\varepsilon_\theta) + n_{I_L}(t_d) \\ Q_L(t_d) &= \sqrt{C}R_L(\varepsilon_\tau)sinc(\pi\Delta f T_p)\sin(\varepsilon_\theta) + n_{Q_L}(t_d) \end{aligned} \quad (8)$$

$n_{I_H}, n_{Q_H}, n_{I_L}, n_{Q_L}$ are independent Gaussian noises. The expression of their variance can be expressed here :

$$\sigma^2_{n_{I_H}} = \sigma^2_{n_{Q_H}} = R_{n_{I_H}}(0) = \frac{N_0}{4T_p}R_{r_{f_H}}(0) \quad (9)$$

$$\sigma^2_{n_{I_L}} = \sigma^2_{n_{Q_L}} = R_{n_{I_L}}(0) = \frac{N_0}{4T_p}R_{r_{f_L}}(0)$$

$R_{r_{f_H}}(\tau)$ and $R_{r_{f_L}}(\tau)$ are the autocorrelation functions of the reference signals filtered respectively by the upper band filter $h_H(t)$ complex conjugate and the lower band filter $h_L(t)$ complex conjugate.

This technique could offer advantages in presence of interference but in general condition, it is unfavorable. First, complexity is increased because two filters has to be set instead of one in classical receivers. Moreover, the use of two filter induce unacceptable error due to filtering effect on the signal. This last issue is discussed later in "Filtering Effect" part.

**"BPSK-like" technique**

The "BPSK -like" technique presented in [1] propose to process the signal in a slightly different manner than the technique seen before. In fact, to get a correlation function whose shape is unambiguous, it is not necessary to filter independently the two principal lobes of the signal. Instead of this, it is possible to use only one centered filter with a bandwidth including the two principal lobes of the spectrum and the secondary lobes between the principal lobes. Two correlation channels are generated : one gives the filtered signal demodulated by a carrier frequency $(F_{carrier} + F_{sc})$ and correlated with a BPSK signal consisting only of the code (right channel), and the second gives the filtered signal demodulated by a carrier frequency $(F_{carrier} - F_{sc})$ and correlated with a BPSK signal consisting only of the code (left channel). Then, the two channels are combined. The principles of this technique is shown on Figure 2 (only left channel is presented). Calculations

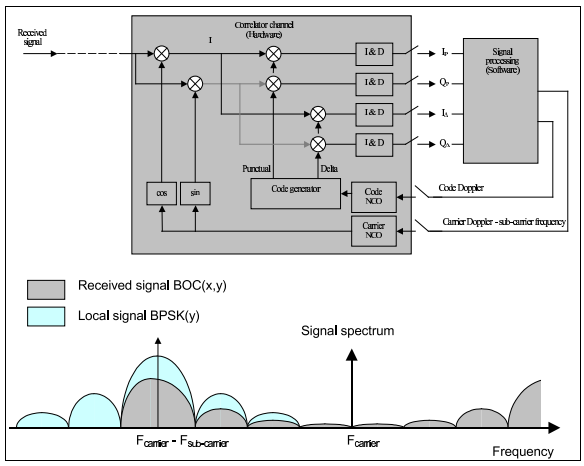


Figure 2: BPSK-like principle

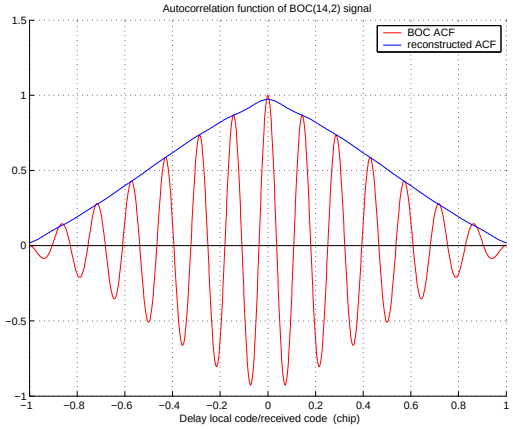


Figure 3: ACF of a BOC(14,2) vs reconstructed ACF

done in previous part still applied here with :

$$h_H(t) = h_L(t) = h(t) \tag{10}$$

where $h(t)$ is a filter which bandwidth include the two principal lobes of the received BOC signal and the secondary lobes within the principal lobes. Figure 3 shows the correlation function on the left channel. We note that the reconstructed ACF by the BPSK-like technique has the expected unambiguous shape. The advantage of the technique is an increased simplicity of the implementation, and above all, the least effect of the filtering.

## THE SUB CARRIER PHASE CANCELLATION METHOD

The Sub Carrier Phase Cancellation technique (SCPC), allows ones to make a non ambiguous acquisition of a BOC signal. Figure 4 present the general principle. The idea here is to get rid of the sub carrier signal as it is done for the carrier signal. In addition to the local in phase and quadrature carrier signals, an in phase and a quadrature local sub carrier signals have to be generated. Thus, two correlation channels are generated here. On one channel, the received filtered signal is correlated with the local BOC signal in sub carrier phase, and on the other one the received filtered signal is correlated with the local BOC signal in sub carrier quadrature. When these two correlation channels are combined, an ACF similar to the BPSK one is obtained. On Figure 5 is shown the correlation obtained on the two channels and the reconstructed ACF when these two correlation functions are squared and summed.

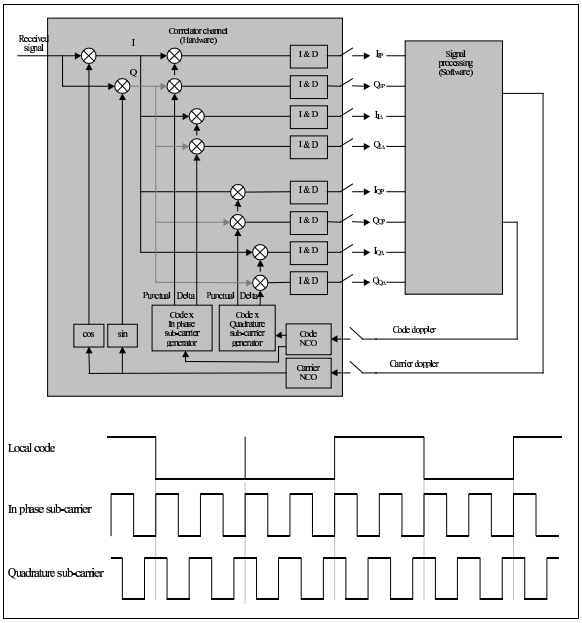


Figure 4: Sub Carrier Phase Cancellation principle

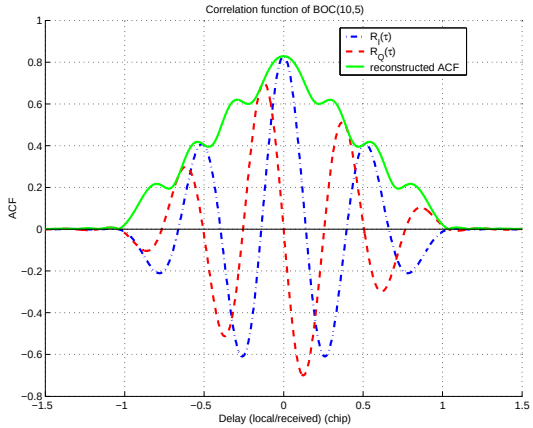


Figure 5: Correlation functions of the received BOC(10,5) code with the in phase and with the quadrature phase sub carrier component

The expression of the local signal $r_I$, in-phase subcarrier signal, and $r_Q$, in quadrature subcarrier signal are detailed as follows:

$$\begin{aligned} r_I(t-\hat{\tau}) &= c(t-\hat{\tau}).sc_I(t-\hat{\tau}) \\ &= c(t-\hat{\tau}).sc(t-\hat{\tau}) \\ r_Q(t-\hat{\tau}) &= c(t-\hat{\tau}).sc_Q(t-\hat{\tau}) \\ &= c(t-\hat{\tau}).sc(t-\hat{\tau}-\frac{T_{sp}}{4}) \end{aligned}$$

We keep the same notations as in the previous section. We note the received filtered BOC signal :

$$s'_f(t) = [(c.sc) * h](t) \tag{11}$$

At the output of the correlator, we get :

$$\begin{aligned} Y_I(t_d) = \frac{1}{T_p}\int_{t_d-T_p}^{t_d} \sqrt{C}s'_f(t-\tau)e^{j\phi(t)}.r_I(t-\hat{\tau})e^{j\hat{\phi}(t)}dt \\ +n_{Y_H}(t_d) \end{aligned} \tag{12}$$

$$\begin{aligned} Y_Q(t_d) = \frac{1}{T_p}\int_{t_d-T_p}^{t_d} \sqrt{C}s'_f(t-\tau)e^{j\phi(t)}.r_Q(t-\hat{\tau})e^{j\hat{\phi}(t)}dt \\ +n_{Y_L}(t_d) \end{aligned}$$

with :

$$\hat{\phi(t)} = -2\pi\hat{f_D}t - \hat{\theta} \tag{13}$$

After the same calculations as in previous section, one can write the expression of the signals on each channel :

$$\begin{aligned} I_I(t_d) &= \sqrt{C}\sin c(\pi\Delta f T_p)\cos(\varepsilon_\theta)R_I(\varepsilon_\tau) + n_{I_I}(t_d) \\ Q_I(t_d) &= \sqrt{C}\sin c(\pi\Delta f T_p)\sin(\varepsilon_\theta)R_I(\varepsilon_\tau) + n_{Q_I}(t_d) \\ I_Q(t_d) &= \sqrt{C}\sin c(\pi\Delta f T_p)\cos(\varepsilon_\theta)R_Q(\varepsilon_\tau) + n_{I_Q}(t_d) \\ Q_Q(t_d) &= \sqrt{C}\sin c(\pi\Delta f T_p)\sin(\varepsilon_\theta)R_Q(\varepsilon_\tau) + n_{Q_Q}(t_d) \end{aligned} \tag{14}$$

with :

$$R_I(\varepsilon_\tau) = \frac{1}{T_p}\int_{t_d-T_p}^{t_d} s'_f(t-\tau).r_I(t-\hat{\tau})dt \quad (15)$$

$$R_Q(\varepsilon_\tau) = \frac{1}{T_p}\int_{t_d-T_p}^{t_d} s'_f(t-\tau).r_Q(t-\hat{\tau})dt$$

And we note $R_I(\varepsilon_\tau)$ the cross-correlation function of the filtered received BOC code with the local in phase BOC code; and $R_Q(\varepsilon_\tau)$ the cross-correlation function of the filtered received BOC code with the local quadrature BOC code. $h(t)$ is the impulse response of the front end filter, which bandwidth is at least of $(2f_{sp}+2f_c)$ (width of the two main lobes BOC spectra). $n_{I_I}, n_{Q_I}, n_{I_Q}, n_{Q_Q}$ are four independent Gaussian noises. As previously, we calculate their variance :

$$\sigma^2_{n_{I_I}} = \sigma^2_{n_{Q_I}} = R_{n_{I_I}}(0) = \frac{N_0}{4T_p}R_{r_{f_I}}(0) \quad (16)$$

$$\sigma^2_{n_{I_Q}} = \sigma^2_{n_{Q_Q}} = R_{n_{I_Q}}(0) = \frac{N_0}{4T_p}R_{r_{f_Q}}(0)$$

$R_{r_{f_I}}(\tau)$ and $R_{r_{f_Q}}(\tau)$ are the autocorrelation functions of the filtered reference in subcarrier phase and in subcarrier quadrature signals.

## THE BUMP JUMPING METHOD

This method suggested by P. Fine and W. Wilson in [6], aims at determining whether or not the peak being tracked is the correct one. It consists in measuring and comparing the received power of adjacent peaks with respect to currently tracked peak and jumping one peak apart left or right depending on the comparison result, until maximum is found. In addition of the three correlation channels present in a typical code loop, Early, Late an Punctual, this algorithm uses also two correlation channels : Very Early ($VE$) and Very Late ($VL$). The Early and Late correlators are used in a code loop to track one peak. The $VE$ and $VL$ correlators which monitor the amplitude of the two peaks close to the Punctual one are translated by one half subcarrier period on each side of the tracked peak. In fact, the algorithm achieves the amplitude comparison with the help of a simple up/down counter mechanism. After each integrate-and-dump period, the absolute values of $VE$, $P$, and $VL$ in-phase samples are compared. If either the $VE$ or $VL$ sample is the largest, then the appropriate counter is incremented and the other one is decremented. If the P sample is the largest, then both the $VE$ and $VL$ counter are decremented. Neither counter is decremented below zero; and when either counter reaches a particular threshold, T, the tracker is jumped to the new peak, and the counters are reset to zero.

The theoretical analysis of this algorithm is intricate because of the use of counters that inputs non-linearity. Moreover, the independence hypothesis of the noises on $VE$, $P$

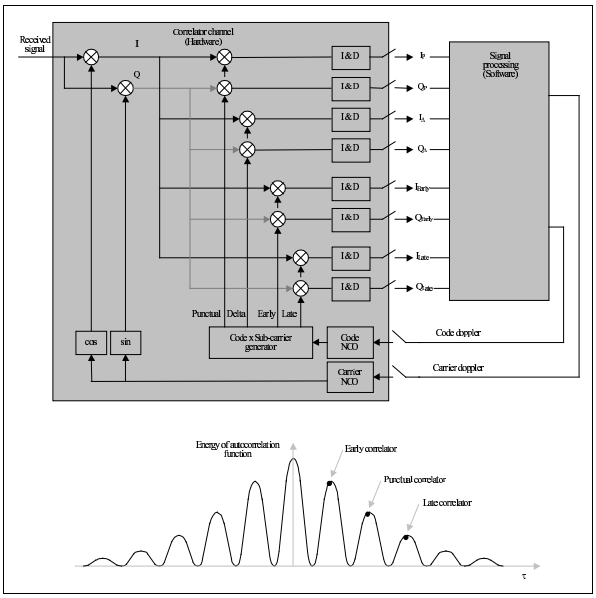


Figure 6: Bump-Jumping principle

and $VL$ channels done in [6] is not assured which complicate the calculations. So, in order to make the study easier, the Bump Jumping (noted BJ) has been seen here through a slightly different angle. The three correlation channels present in a typical code loop, Early, Late an Punctual are kept. Thanks to an Early minus Late power discriminator, the receiver is assumed to lock on the maximum of a peak of the BOC ACF. Then, instead of using counters, it has been considered that the "jumps" from a secondary peak to the central one is done using a discriminator formed with $VE$ and $VL$ correlator channel outputs. This discriminator is of type (see Figure 7 ):

$$D_{BJ1} = VE^2 - VL^2 \quad (17)$$

Since the VE and VL correlators are positioned at half sub-

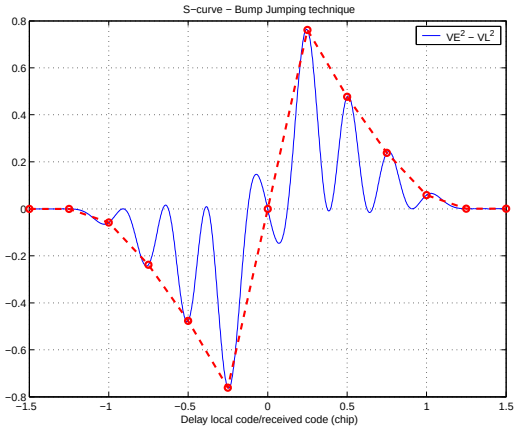


Figure 7: Bump-Jumping discriminator

carrier wave length distance from the P correlator, which

is assumed to be locked on a peak thank to the code loop based on $E$ minus $L$ power discriminator, the $VE$ minus $VL$ power discriminator works only on the circled points on Figure 7.

Another point is that the Bump-Jumping algorithm can not be used in energy search mode. But, the $VE$ or $VL$ correlation channel already set could be used to recover a non ambiguous energy function. Indeed, if the $VE$ and $P$ (or the $VL$ and $P$) samples are combined, the resulting energy function is no more annulling in the interval $[-T_c, T_c]$ (see Figure 8). Thus any risk of missed detection due to zero crossing of the correlation function is avoided.
In fact, this method is very close to SCPC technique since for SCPC technique two correlators in subcarrier phase and in quadrature subcarrier phase are used and for $VE + P$ technique two correlators separated by a time equal to $T_{sc}/4$ are used. Indeed, the local signals for SCPC technique are :

$$\begin{aligned} r_I(t-\hat{\tau}) &= c(t-\hat{\tau}).sc(t-\hat{\tau}) \\ r_Q(t-\hat{\tau}) &= c(t-\hat{\tau}).sc(t-\hat{\tau}-\frac{T_{sp}}{4}) \end{aligned}$$

and for $VE + P$ technique, the local signals are :

$$\begin{aligned} r_P(t-\hat{\tau}) &= c(t-\hat{\tau}).sc(t-\hat{\tau}) \\ r_{VE}(t-\hat{\tau}) &= c(t-\hat{\tau}-\frac{T_{sp}}{4}).sc(t-\hat{\tau}-\frac{T_{sp}}{4}) \end{aligned}$$

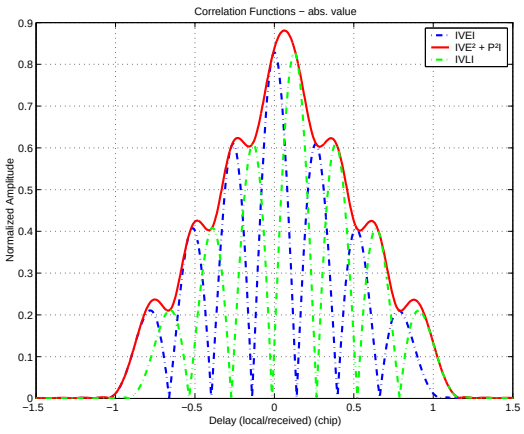


Figure 8: Combined signals for energy search

## FILTERING EFFECTS

To this point, Figures of correlation functions were obtained assuming ideal filtering. In order to be more realistic, we now study the effect of a non ideal filter with a non constant time group delay. The filters used here are Butterworth filters. Figure 9 shows the autocorrelation function of the BOC signal and the correlation function using Dual Side Band method for which two filters are used. Not only the filtering induces a translation on the correlation functions due to the time group delay, but as far as this last one is non constant over the frequency band of the signal, it makes the code of the signal unsynchronized with the subcarrier. It can be noticed that the maximum of the correlation functions are not located at a zero delay value. It implies a residual error in the receiver which can be corrected by a smart calibration of the filters. Above all, the unsynchronization between the code and the subcarrier, due to the use of two filters with too narrow bandwidths, can well be observed on Figure 9 (bandwidth of $12.276MHz$). Indeed, the correlation function reconstructed is no more coincident with the correlation function of the nominal BOC signal. Thus, at the end of the transition to tracking stage, the code loop will be locked at the point corresponding to the maximum of the Dual Side Band technique ACF. Then the receiver will switch to nominal full BOC tracking based on the BOC nominal ACF and lock on a secondary peak providing an unacceptable error. This technique could be possibly useful when an interfence is present on one lobe of BOC signal. Otherwise, "BPSK-like" technique has to be preferred.

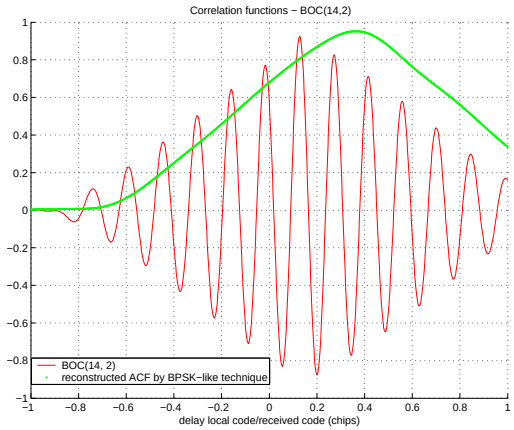


Figure 9: Impact of the filter on the ACF - $BW = 12.276MHz$

Indeed, Figure 10 shows the ACF of full BOC(14,2) versus reconstructed ACF by BPSK-like technique using a Butterworth filter of order $10$ and bandwidth $32.736MHZ$ (corresponding to the band including the principal lobes of the signal spectrum and the secondary lobes in-between). It can be seen that "BPSK-like" let us to get rid of the problem of unsynchronization between the code and the subcarrier. The correlation function reconstructed by BPSK-like technique is well coincident with the correlation function of the nominal BOC signal. Moreover the envelope is sharper at its maximum than previous technique. So, risks of wrong peak selection is avoided. If the bandwidth of the filter is reduced, the correlation losses increase but the

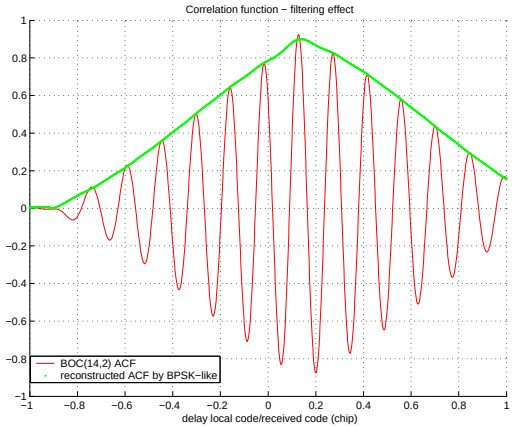


Figure 10: ACF of full BOC(14,2) vs reconstructed ACF

correlation function reconstructed by BPSK-like technique and the correlation function of the nominal BOC signal are still coincident.
Nevertheless, for some types of filter, the solving of the BOC ambiguities issue is not assured. Figure 11 has been obtained with Butterworth filters of order 14 and bandwidth $28.644MHz$. It can be noticed that at its maximum the reconstructed ACF is more flat, and the shape of the nominal BOC ACF under the envelope has changed. The two highest peak of this last one are very close in amplitude. Thus, when switching to transition to tracking stage, there is a risk of locking on the secondary peak inducing an error.

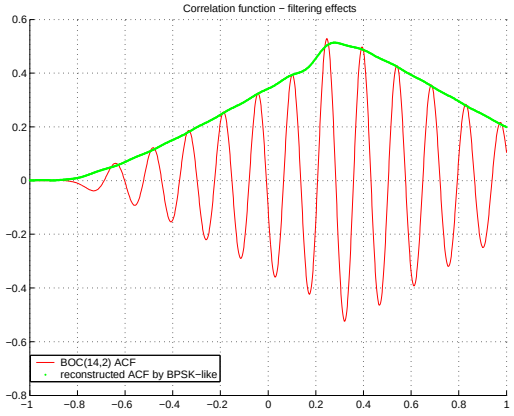


Figure 11: ACF of full BOC(14,2) vs reconstructed ACF

On Figure 12 has been plotted the BOC (14,2) ACF and the ACF obtained with SCPC technique. The filter employed has the same characteristics than the one used to plot Figure 10 : Butterworth filter of order 10 and of bandwidth $32.736MHz$. As expected, we note that the filter induces a translation on the correlation functions due to the time group delay. And, as it is the case with the BPSK-like technique, the enveloppe reconstructed by the Sub Carrier Phase Cancellation technique is still coincident with the

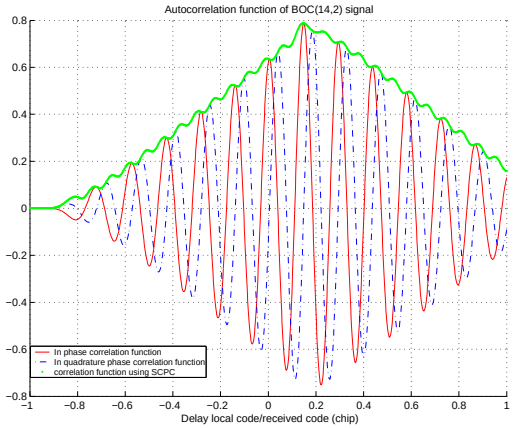


Figure 12: Carrier cancellation technique-Filtering effects

correlation function of the nominal BOC signal. Thus, any risk of wrong peak selection at the end of the transition to tracking stage is avoided. If at the end of the transition to tracking stage the receiver is locked on the maximum of the envelope, when switching to tracking stage, the receiver will lock on the maximum of the central peak of the BOC correlation function.

It has been plotted on Figure 13 the two discriminators

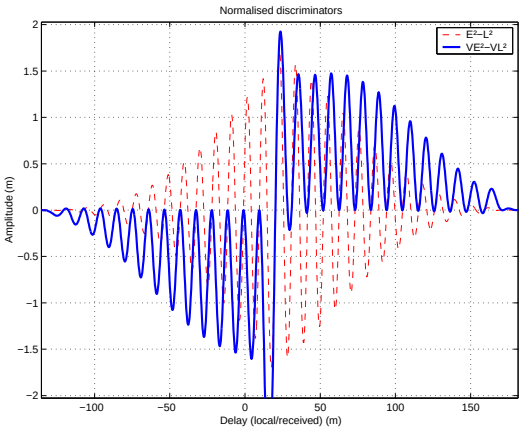


Figure 13: Bump-Jumping technique-Filtering effects

used for Bump-Jumping technique, in the same filtering conditions. The two discriminators curves are perfectly coincident, and a false lock at the end of the transition process is not worrying.
As before, for some types of filter, the solving of the BOC ambiguities issue could be less obvious. But for the three techniques, non ambiguous acquisition remains feasible for a large range of filter's orders and filter's bandwidths.
To conclude, the three techniques show the same performance with respect to filtering effect.

## ENERGY SEARCH

The acquisition process is a two-dimensional (in time

and frequency) search over an uncertainty region. The signal detection is based on a hypothesis test. Under hypothesis **H0**, the useful signal is considered absent. Under hypothesis **H1**, the useful signal is considered present. The statistic test is compared to a threshold and the decision of considering the signal acquired or not is made with a certain probability of detection, $P_d$, and false alarm probability, $P_{fa}$. The acquisition strategy studied here is the single dwell time search described in [7] [8]. A trial integration of $\tau_D$ is made on the received signal, i.e. $N_{nc}$ samples of the four channels' output are non-coherently summed. $N_{nc}$ is the number of non-coherent integration, $\tau_D$ is the dwell time, and if $T_P$ is the coherent integration time, we have : $\tau_D = N_{nc}.T_P$. If the threshold ($S_{acq}$) is not exceeded, then the reference code is delayed. We continue to sweep the uncertainty region until a hit occurs, i.e. threshold is exceeded. Then it turns to a verification, without changing the code phase, that may be an entry into a code tracking loop. The signal is then considered being acquired.
The energy search method is the same for the three methods studied in this paper. Since these three methods use four correlator channels to solve the BOC ambiguities problem, the samples of the four channels' output are called $I_1(k)$, $Q_1(k)$, $I_2(k)$, $Q_2(k)$. The 1 index refers to $H$, $I$, or $VE$ and the 2 index refers to $L$, $Q$, or $P$ respectively if the BPSK-like, the SCPC or $VE$ plus $P$ power technique is used.
Although, for calculations, the signals have been previously assumed continuous, sampled versions of these signals is used here.
Under hypothesis **H0** (signal is not present), the statistic test is :

$$T_0 = \sum_{k=1}^{N_{nc}} [n_{I_1}(k)^2 + n_{Q_1}(k)^2 + n_{I_2}(k)^2 + n_{Q_2}(k)^2] \quad (18)$$

$\frac{T_0}{\sigma_n^2}$ is a central $\chi^2$ distribution with $4Nnc$ degrees of freedom, called here $p_{T_0}$. The false alarm probability is then expressed by :

$$P_{fa} = Pr[T_0 > Sacq] = \int_{S_{acq}}^{\infty} p_{T_0}(\lambda) d\lambda = f(Sacq) \quad (19)$$

Under hypothesis **H1** (signal present), the test statistic is :

$$T_1 = \sum_{k=1}^{N_{nc}} [I_1(k)^2 + Q_1(k)^2 + I_2(k)^2 + Q_2(k)^2] \quad (20)$$

$\frac{T_1}{\sigma_n^2}$ is a noncentral $\chi^2$ distribution with $4Nnc$ degrees of freedom, called here $p_{T_1}$.
The non centrality parameter is :

$$\Theta = \frac{4C}{N_0} N_{nc} T_p \sin c(\pi \Delta f T_p)^2 . \frac{[R_1(\varepsilon_\tau)]^2 + [R_2((\varepsilon_\tau)]^2}{R_{r_{f_1}}(0)} \quad (21)$$

The detection probability is then expressed by :

$$P_d = Pr[T_1 > Sacq] = \int_{Sacq}^{\infty} p_{T_1}(\lambda) d\lambda \quad (22)$$

The mean acquisition time can be deduced from the calculations above. In [7], one indicates the single dwell time search process mean acquisition time is :

$$\overline{T_{acq}} = \frac{2 + (2 - P_d)(N_t - 1)(1 + k_p P_{fa})}{2P_d} T_p N_{nc} \quad (23)$$

where :
$P_d$ is the probability of detection
$P_{fa}$ is the false alarm probability
$N_t$ is the uncertainty region size
$T_p$ is the coherent integration time
$N_{nc}$ is the non coherent integration number
$k_p$ is the penalty factor. It corresponds to the time lost if a false alarm occurs.

In the Simulation part detection probability and mean acquisition time are plotted and compared to results obtained by Monte-Carlo simulations.

## TRANSITION TO TRACKING

Once the energy is found, the acquisition process closes a code loop in order to make the local code phase converging toward the received code, based on the same correlation scheme. In this part, we give the expression of the closed loop error variance in transition to tracking mode. Assuming the code loop is affected by Gaussian noise which power spectral density is flat across the loop bandwidth, Holmes shows in [7] that the variance of the error of synchronization expressed in squared units of chips is given by :

$$\sigma_{\varepsilon_\tau}^2 = E\left[\frac{\varepsilon_\tau^2}{T_c^2}\right] = \frac{2B_L T_p R_N(0)}{(K.T_c)^2} \quad (24)$$

where:
$B_L$ is the one sided closed loop bandwidth of the code tracking loop
$T_p$ is the coherent integration time
$K$ is the discriminator gain
$T_c$ is the chipping period
$R_N(0)$ is the autocorrelation of the noise at the output of the integrator, i.e the noise power.
Thus the calculation of the closed loop tracking error variance is reduced to evaluating the noise correlation at zero and evaluating the gain of the discriminator. This paper focuses on transition to tracking mode where techniques to make the ACF unambiguous are used. In this stage, the remaining delay uncertainty after acquisition is solved. After this transition, the estimated delay is likely within the pull-in range of the code tracking loop. Expressions of the closed loop error variance in tracking mode are given in [9].

For this study, the discriminator used for BPSK-like and SCPC techniques is a Dot Product. Three correlators for each channel previously described are set : a Ponctuel, an Early, and a Late one. The error signal at the output of this discriminator has the expression :

$$V_{dotP} = I_{P1}.(I_{E1} - I_{L1}) + Q_{P1}.(Q_{E1} - Q_{L1}) \quad (25)$$
$$+I_{P2}.(I_{E2} - I_{L2}) + Q_{P2}.(I_{E2} - Q_{L2})$$

As before, the 1 index refers to $H$, or $I$ and the 2 index

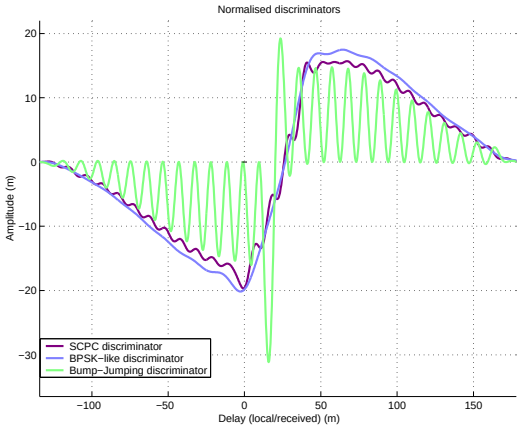


Figure 14: Normalized discriminator of the three techniques

refers to $L$, or $Q$ respectively if the BPSK-like, or the SCPC is used. The chip spacing between the correlators is named $\delta$.
For Bump-Jumping technique, as it is previously described, two combined discriminators are used :

$$V_{EmLP} = E^2 - L^2 \quad (26)$$
$$V_{VEmVLP} = VE^2 - VL^2 \quad (27)$$

It is assumed here that the Doppler error is solved : $\Delta f = 0$. And we get for the three techniques :

$$V(\varepsilon_\tau) = C\left[S_{ig}(\varepsilon_\tau)\right] + \sqrt{C}\left[N_{1^{rst}order}\right] + N_{2^{nd}order}$$

$S_{ig}$ is the signal term, $N_{1^{rst}order}$ is the first order noise term (product of the noise and the signal),and $N_{2^{nd}order}$ is the second order noise term (product of the noise by the noise). The expression of the discriminator gain is :

$$K = C\frac{\partial}{\partial \varepsilon_\tau}\left[S_{ig}(\varepsilon_\tau)\right]|_{\varepsilon_\tau=0} \quad (28)$$

The discriminator curves and the first and second order noise affecting the discriminators has been plotted on Figure 15 for the three techniques. In order to compare the techniques, the curves on this Figure has been normalized by the gain $K$. With respect to the noise, the three

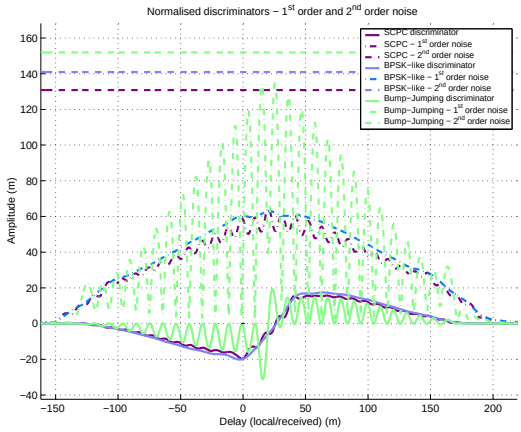


Figure 15: Normalized discriminator of the three techniques vs $1^{st}$ and $2^{nd}$ order noises

techniques seem to shows approximately the same performance.

Finally, we give the expression of the standard deviation of the tracking error (in meter) :

$$\sigma_\varepsilon = c.\sqrt{\frac{B_L}{2C/N_0}\frac{1}{\mu^2}\left[\sigma_1 + \frac{\sigma_2}{T_p.C/N_0}\right]} \quad (29)$$

with :

$$\sigma_1 = R_{r_{f_1}}(0).\left[(R_1(\varepsilon_\tau+\delta) - R_1(\varepsilon_\tau-\delta))^2 + 2R_1^2(\varepsilon_\tau)\right]$$
$$+R_{r_{f_2}}(0).\left[(R_2(\varepsilon_\tau+\delta) - R_2(\varepsilon_\tau-\delta))^2 + 2R_2^2(\varepsilon_\tau)\right]$$
$$-2R_{r_{f_1}}(2\delta)R_1^2(\varepsilon_\tau) - 2R_{r_{f_2}}(2\delta)R_2^2(\varepsilon) \quad (30)$$

$$\sigma_2 = R_{r_{f_1}}(0)\left[R_{r_{f_1}}(0) - R_{r_{f_1}}(2\delta)\right] \quad (31)$$
$$+R_{r_{f_2}}(0)\left[R_{r_{f_2}}(0) - R_{r_{f_2}}(2\delta)\right]$$

$$\mu = \frac{\partial}{\partial \varepsilon_\tau}[R_1(\varepsilon_\tau)\left(R_1(\varepsilon_\tau+\delta) - R_1(\varepsilon_\tau-\delta)\right) \quad (32)$$
$$+R_2(\varepsilon_\tau)(R_2(\varepsilon_\tau+\delta) - R_2(\varepsilon_\tau-\delta))]|_{\varepsilon_\tau=0}$$

$\sigma_1$, $\sigma_2$, $\mu$ are numerically computed. In Simulation part the standard deviation of the tracking error is plotted in order to compare BPSK-like and SCPC techniques. The time spent in transition to tracking has also been evaluated to compare Bump-Jumping technique with the two other ones. Indeed, Figure 16 describes the type of code tracking loop used in transition to tracking stage. With this type of loop scheme, it can be asserted that the code loop standard deviation is proportional to the time elapsed in transition to tracking stage. And, in order to avoid any false lock, one must have at the end of the transition process:

$$3.\sigma_{\epsilon_\tau} \leq \frac{\lambda_{sc}}{4} \quad \text{with} \quad \lambda_{sc} = \frac{c}{f_{sc}} \quad (33)$$

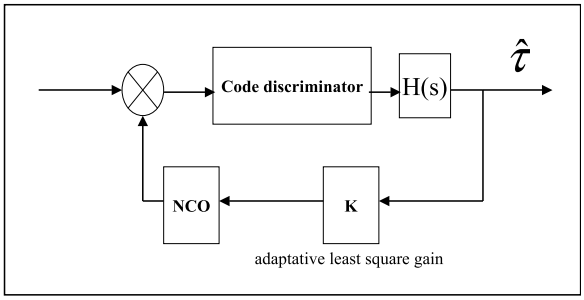


Figure 16: Code loop principle scheme

Thus, the minimum time spent in transition ($T_{trans}$) can be deduced from 33.

## SIGNAL ACQUISITION PERFORMANCE RESULTS

The simulations done in order to assess the performance of each method previously presented, can be divided in two parts : simulations of the energy search and simulations of the transition to tracking stage. For simulations of energy search, a PRN Gold Code of length $1023$ has been used. The coherent integration time $T_p$ is equal to $1ms$. The type of energy search chosen is aided acquisition, i.e all code bins are searched, but only one frequency cell is supposed to be searched. A half-chip rate is used to search the code bins. An error Doppler of $250Hz$ has been taken into account, which is the maximum frequency error associated with the coherent integration time chosen.
First the false alarm probability is set to $10^{-3}$. By solving equation 19, the detection threshold can be computed. Then, Monte-Carlo simulations of the energy search process has been done to produce the detection probability for different value of $N_{nc}$ chosen. The signals are assumed to be corrupted only by white Gaussian noise. The filter used are $10$ order Butterworth filter of bandwidth : $B_F = 2f_{sc} + 2f_c$.

### Energy search

Figure 17 shows the detection probability and the false alarm probability for a BOC(10,5) when using the sub-carrier phase cancellation technique. The not solid lines represent the theoretical detection probability from equations 22 and 21. It could be noticed that except for low values of $C/N_0$, simulated detection probabilities well agree with theoretical ones. Figure 18 illustrates the difference between detection probability for a BOC(10,5) and a BOC(14,2). At equal value of $Pd$ a difference of $3dBHz$ on the $C/N_0$ can be read.

Again, on Figure 19 and 20 have been plotted the detection probability for a BOC(10,5) when using respectively the BPSK-like technique and the technique combining the $VE$ and $P$ correlations. On Figure 21, the three techniques have been compared for a BOC(10,5) and a number of non-coherent integration of $Nnc = 50$. It can be noticed that

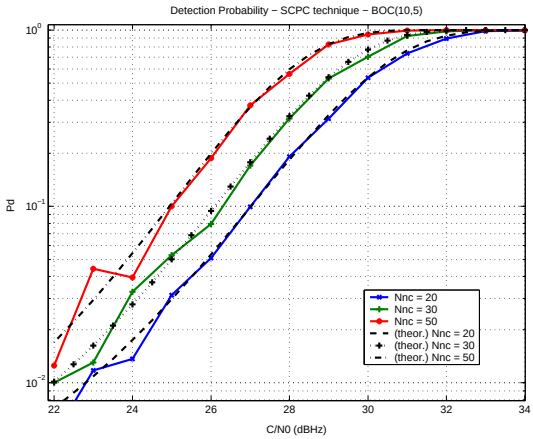


Figure 17: Pd and Pfa for a BOC(10,5) using SCPC

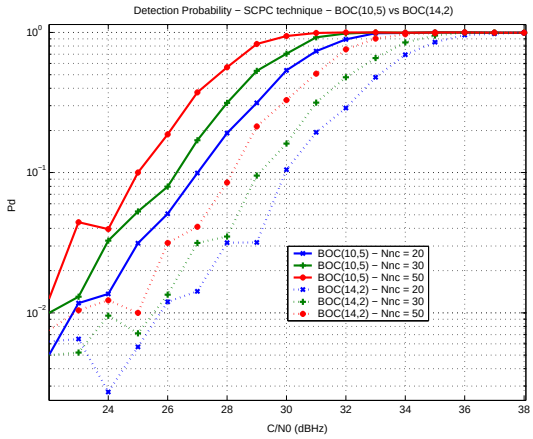


Figure 18: Pd for a BOC(10,5) and a BOC(14,2) using SCPC

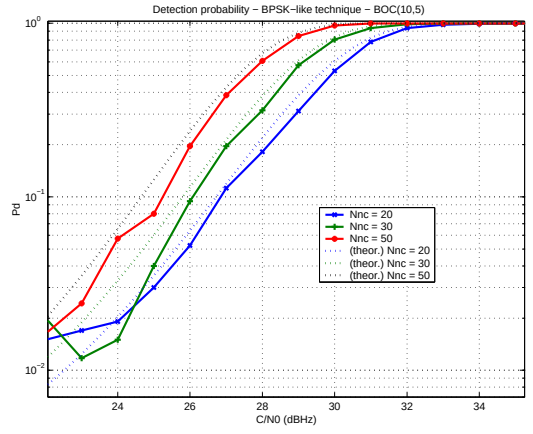


Figure 19: Pd for a BOC(10,5) using BPSK-like

they provide hardly the same detection probability. At low $C/N_0$, the technique combining $VE$ and $P$ correlations presents a little improvment (a difference almost equal to $0.5dBHz$).

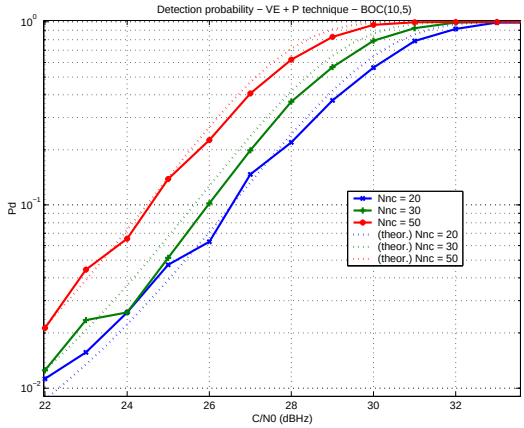


Figure 20: Pd for a BOC(10,5) - technique combining the $VE$ and $P$ correlations

Naturally, it has to be noticed that increasing the bandwidth of the filter would improve the performance of the methods. Figure 22 shows the single dwell search process

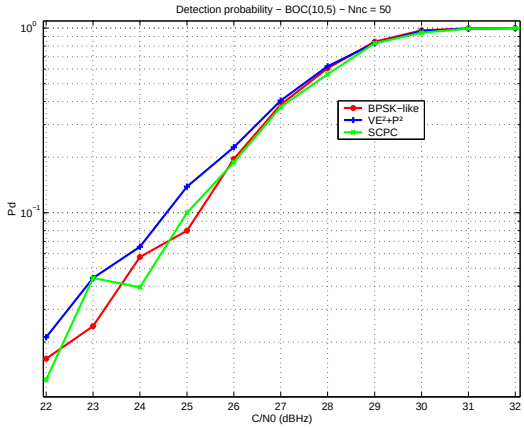


Figure 21: Pd for a BOC(10,5) - comparison of the three techniques

mean acquisition time versus $C/N_0$ for the three different methods. Here again, BPSK-like and SCPC techniques shows approximately the same performance although the technique combining $VE$ and $P$ correlations presents an little improvement particularly at low $C/N_0$.
The asymptotic mean acquisition time is $31.8s$.

**Transition to tracking**

The standard deviation of the code tracking error for the BPSK-like et and for the Sub Carrier Phase Cancellation techniques has been plotted on Figure 23 in transition stage.
As a comparison, the standard deviation of the code tracking error for a BPSK signal is shown too (approximated expression from [9]). It can be noticed that BPSK-like et Sub Carrier Phase Cancellation techniques are close with

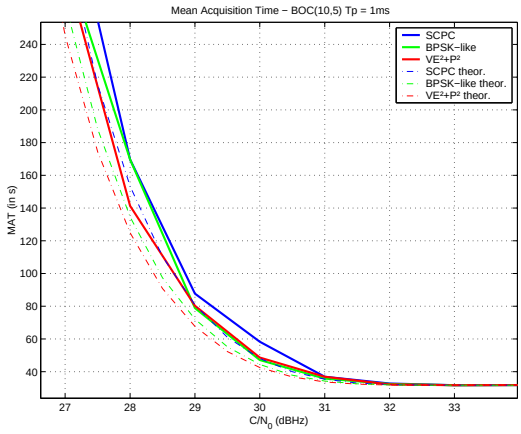


Figure 22: Mean Acquisition Time for a BOC(10,5) - comparison of the three techniques

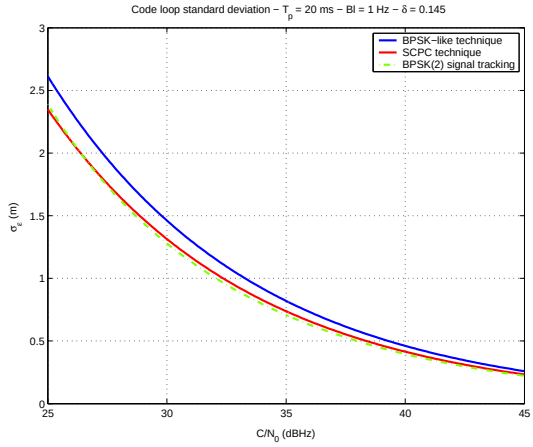


Figure 23: Standard deviation in transition to tracking stage

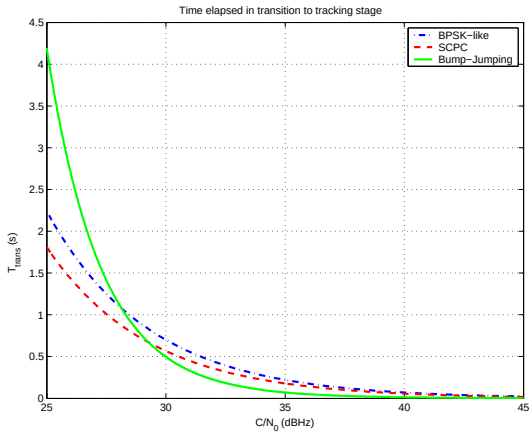


Figure 24: Time to transit to tracking stage

respect to standard deviation. But Sub Carrier Phase Cancellation technique provides a significative improvement.
Figure 24 shows the time elapsed in transition to tracking stage in order to obtain the desired accuracy. It has

been plotted for BOC(14, 2) signal. One can see that for Bump-Jumping technique this time is higher for low values of $C/N_0$ than for the two other techniques. For greater $C/N_0$, this trend is reversed, Bump-Jumping seems to be better. But, for Bump-Jumping technique, the time $T_{trans}$ plotted is a minimum value since it has been assumed that the algorithm has only to process one "jump" from the closest secondary ACF peak to the central one.

**CONCLUSION**

The performance of three BOC acquisition techniques has been assessed here in two stages of the signal processing. BPSK-like and Sub-Carrier Phase cancellation methods seem to present at least the same performance than Bump-Jumping technique which seems to be a reference. This results was expected since the principle of these three techniques are in fact very close. The study has now to be pursued with the impact of multipath on BOC signal ambiguities issue.

**ACKNOLEDGEMENT**

I wish to thank Nicolas MARTIN from THALES Avionics for his support, his helpful advises, and the simulation tools that his company put at my disposal to carry out this study.

# References

[1] N. Martin, V.Leblond, G. Guillotel, V. Heiries "'BOC (x,y) signal acquisition techniques and performance,"*Proceeding of ION 2003*, Portland, September 2003

[2] Philip M. Fisman,John W. Betz, "'Predicting Performance of Direct Acquisition for the M-Code Signal,"*Proceeding of ION NTM 2000*, Anaheim, January 2000

[3] Brain C. Barker, John W. Betz, John E. Clark, Jeffrey T.Correia, "'Overview of the GPS M Code Signal,"*Proceeding of ION NTM 2000*, Anaheim, January 2000

[4] J. K. Holmes, "Code Tracking Loop Peformance Including the Effects of Channel Filtering and Gaussian Interference,"*Proceeding of the IAIM World congress in association withe U.S. ION Annual Meeting, 26-28 June 2000, San Diego*

[5] J. Winkel, "'Modeling and Simulating GNSS Signal Structures and Receivers,"PhD manuscript, 2000

[6] P. Fine, W.Wilson, "'Tracking Algorithm for GPS Offset Carrier Signals,"*Proceeding of ION 1999*

[7] J. K. Holmes, "'Coherent Spread Spectrum Systems,",1990

[8] F. Bastide, O. Julien, C. Macabiau, B. Roturier "'Analysis Of L5/E5 Acquisition, Tracking, and Data Demodulation Thresholds,"*Proceeding of ION 2002*, Portland, September 2002

[9] L. Ries, L. Lestarquit, E. Armengou-Miret, F. Legrand, W. Vigneau, C. Bourga, P. Erhard, J.L. Issler, "'A Software Simulation Tool for GNSS2 BOC Signal Analysis,"*Proceeding of ION 2002*, Portland, September 2002